Gene Therapy (2000) 7, 1690–1697

www.nature.com/gt



# Supramolecular structure and nuclear targeting efficiency determine the enhancement of transfection by modified polylysines

C-K Chan[1], T Senden[2] and DA Jans[3]
[1]*Nuclear Signalling Laboratory, Division of Biochemistry and Molecular Biology, John Curtin School of Medical Research;* [2]*Research School of Physical Sciences and Engineering, Australian National University, Canberra, Australia*

*Polylysine (pLy) has been used as a DNA carrier in nonviral gene delivery systems because it forms complexes with plasmid DNA via charge interaction, and condenses it into a compact structure. We have recently shown that cross-linking nuclear localization sequences (NLSs) to pLy can enhance transfection by conferring specific recognition by the cellular nuclear import 'receptor', the NLS-binding importin α/β heterodimer. The present study examines and correlates for the first time the effect of the lysine/nucleotide (Ly/Nu) ratio on transfection, recognition by importin α/β, and structure as determined using electron microscopy (EM) and atomic force microscopy (AFM), for pLy–DNA complexes with and without NLSs or mutant versions thereof. Intriguingly, we observed two distinct peaks of transfection enhancement at Ly/Nu ratios of 0.4 and 4.0, attributable to specific NLS recognition by importins and DNA compaction, respectively. The results indicate a clear correlation between the pLy–DNA structure, importin α/β recognition, and gene transfer efficiency, thus underlining the importance of using pLy–DNA at the optimal Ly/Nu ratio.* Gene Therapy (2000) **7,** 1690–1697.

**Keywords:** *nonviral DNA transfer; electron microscopy; atomic force microscopy; nuclear localization signals; importin subunits*

## Introduction

Polylysine (pLy) has been used in nonviral gene delivery because of its ability to form complexes with DNA via charge interaction. Various ligands have been covalently attached to pLy as a means to link these molecules to DNA,[1–6] and thereby effect cell-specific delivery and uptake of plasmid DNA. pLy has been shown to form condensed toroids of 80–100 nm with DNA[1] to confer resistance to DNase,[7] with multi-step condensation reported in the presence of high NaCl concentrations.[8] Condensation of plasmid DNA by pLy appears to correlate with improved gene transfer efficiency.[9–11] Recently, we cross-linked peptides constituting the nuclear localization signal (NLS) of the simian virus SV40 large tumor antigen (T-ag) to pLy, in addition to internalisable ligands, and showed enhancement of gene transfer.[12]

In this study, we examine the effect of complexation of DNA with pLy itself or with pLy to which NLS or mutant NLS peptides are cross-linked[12] at a range of different lysine/nucleotide (Ly/Nu) complexation ratios. We observe a clear correlation between structure and NLS recognition by the cellular nuclear import receptor, the importin α/β heterodimer, and transfection efficiency. Electron microscopic (EM) and atomic force microscopic (AFM) approaches indicate that the tertiary structure of the pLy–DNA complex changes with the Ly/Nu ratio, showing a step-wise collapse, with toroids (*c.* 60 nm) forming at a Ly/Nu of 0.4 and compact beads (*c.* 16 nm) at a Ly/Nu of 4.0, with aggregated matrixes observed at a Ly/Nu of 2.0. We also find transfection to be strongly dependent on the Ly/Nu ratio, with the greatest enhancement afforded by NLS-containing pLy. Transfection efficiency shows distinct peaks at two different Ly/Nu ratios (0.4 and 4.0), corresponding to the specific effects of recognition of the functional NLS and DNA compaction, respectively. Both NLS recognition and DNA compaction are thus important parameters in pLy-enhanced transfection, underlining the importance of using pLy–DNA at the optimal Ly/Nu ratio.

*Correspondence: DA Jans, Nuclear Signalling Laboratory, Division of Biochemistry and Molecular Biology, John Curtin School of Medical Research, Australian National University, 0200, Canberra, Australia*
Received 25 February 2000; accepted 10 June 2000

## Results

The ability of pLy to enhance gene transfer has been attributed to the ability of pLy to form compact particles with DNA.[1] We have previously shown that pLy, when complexed with DNA at a Ly/Nu ratio of 0.4, is not recognised by α/β-importin, in contrast to pLy to which peptides including an optimised T-ag NLS (P101) are covalently cross-linked (pLyP101). We set out to examine importin binding and transfection efficiency rigorously with respect to the Ly/Nu ratio, in the context of the structure and size of the DNA complexes.

### *Ly/Nu-dependent enhancement of transfection by pLy*

The enhancement potential of DNA transfer by pLy and pLy-P101 peptide conjugates was investigated using HTC rat hepatoma cells and calcium phosphate and lipofectamine transfection procedures. Enhancement of transfection above that of DNA alone by pLy, or by pLy to which the non-functional mutant T-ag NLS peptide (P101T) was coupled (pLyP101T), was compared with that effected by pLyP101–DNA complexes over a range of Ly/Nu ratios using either plasmid pSV2neo,[13] which contains the neomycin resistance gene that confers resistance to the antibiotic G418 (stable transfection), or plasmid pCH110[14] which encodes the *Escherichia coli* β-galactosidase enzyme (transient transfection).

Enhancement of transient transfection using both calcium phosphate and lipofection procedures was observed for pLy, pLyP101 and pLyP101T and depended strongly on the Ly/Nu ratio with two maxima (Figure 1). The direct comparison of pLyP101 and pLy is shown in Figure 1a, while a comparison of pLyP101 with pLyP101T is shown in Figure 1b, enhancement of transfection by pLyP101 being *c.* 50–60% higher than that by pLy and pLyP101T, respectively, at the first peak (Ly/Nu ratio of 0.4), indicating that the enhancement of gene transfer by pLyP101 as compared with pLyP101T at a Ly/Nu ratio of 0.4 is attributable to the functional NLS peptide as opposed to the mutant NLS peptide. In contrast, the level of transfection at the second peak (Ly/Nu of 4.0) effected by pLyP101 was comparable to that by pLy and pLyP101T, implying that the effect in this case was distinct from nuclear targeting requirements. A trend similar to that for transient transfection was observed for stable transfection, indicating maximal enhancement at Ly/Nu ratios of 0.4 and 4.0, and with pLyP101 conferring a greater enhancement than pLy or pLyP101T (see below, and results not shown).

Both pLyP101 and pLyP101T contain an identical number of linked peptide (*c.* 30 mol peptide/mol pLy – see Materials and methods), so that the enhancement of transfection by the former, albeit not greater than 60%

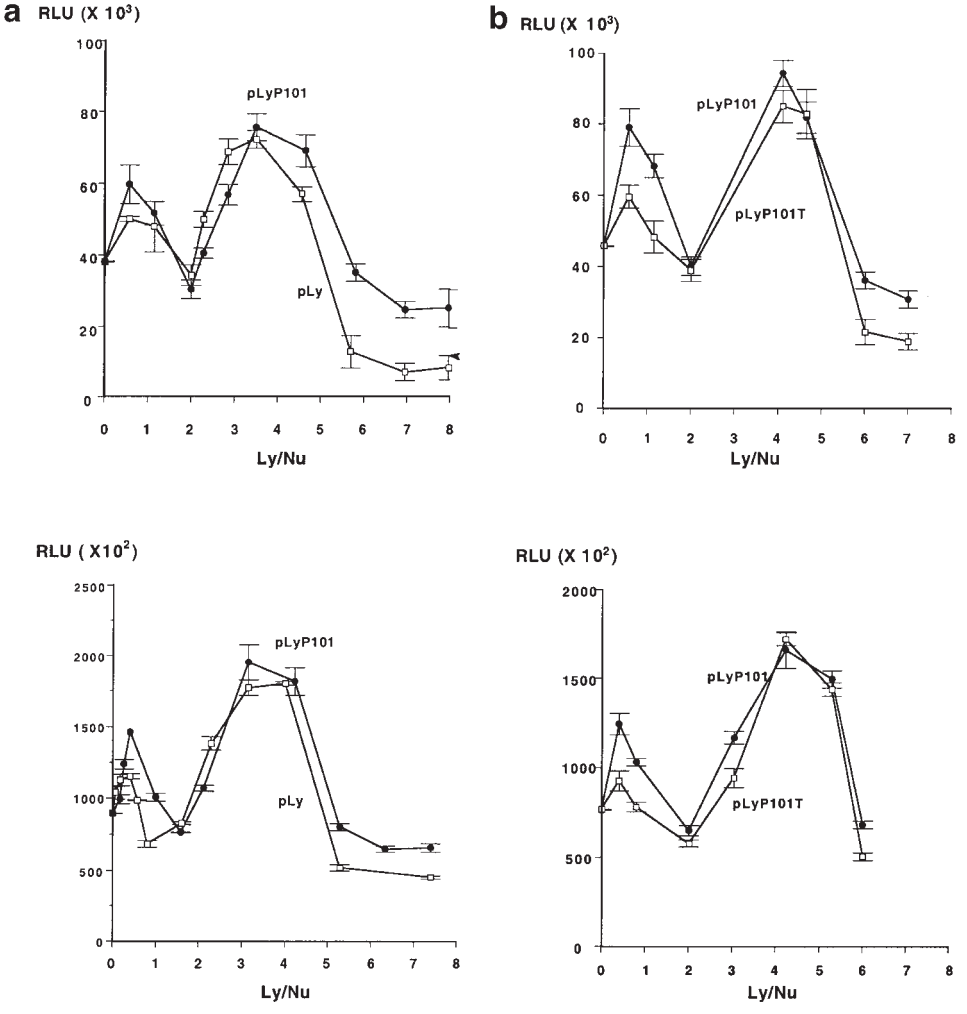


***Figure 1*** *Dependence on Ly/Nu of the efficiency of transient transfection of HTC cells with pLy derivatives using calcium phosphate (top panels) and lipofectAMINE procedures (bottom panels). pLy, pLyP101 and pLyP101T were complexed with 2 μg of pCH110 plasmid DNA at different Ly/Nu ratios before incubation with $CaCl_2$ and BBS buffer and addition to HTC cells (see Materials and methods) for calcium phosphate transfection (top). LipofectAMINE transfection (bottom) was carried out according to the specification of the manufacturer (see Materials and methods). Results for pLyP101 are compared with those of pLy (a) and pLyP101T (b); experiments were performed on different days. β-galactosidase activity of HTC cells was analysed 48 h after transfection using a chemiluminescence assay (TROPIX, see Materials and methods) with the results ± s.e.m. (n = 3) expressed as RLU (relative light unit) corrected for protein content in cell extracts.*

even at a Ly/Nu of 0.4, is directly attributable to the effect of the functional NLS, rather than differences in cross-linking efficiency etc. pLy derivatives with lower numbers of cross-linked P101 peptide gave lower enhancement of transfection (data not shown), consistent with the conclusion that the NLS of P101 was responsible for the ehancement of transfection. Despite the fact that pLyP101 was superior in its ability to enhance both transient and stable transfection, pLy and pLyP101T also clearly improved transfection efficiency, relative to in their absence (ie DNA alone). This was consistent with pLy's documented DNA compaction properties,[1] but the finding that the enhancement of transfection had maxima at two distinct Ly/Nu ratios was truly novel.

### *Importin binding and nuclear import of pLy derivatives*

To ascertain the efficacy of pLyP101 over pLy and pLyP101T in its ability to target DNA to the nucleus through conferring interaction with the cellular nuclear transport machinery, recognition of pLy, pLyP101 and pLyP101T with and without complexed DNA by the NLS-binding mouse α/β-importin heterodimer (mIMPα/β) was assessed using an established ELISA-based assay.[15] pLy, pLyP101 and pLyP101T without DNA were all recognised by mIMPα/β with pLyP101 having higher binding affinity and maximal binding (see Figure 2). When the conjugates were complexed with plasmid DNA (at Ly/Nu = 0.4), the binding affinity and maximal binding of all three conjugates decreased (see Figure 2), pLy and pLyP101T–plasmid DNA complexes showing negligible binding. In contrast, the pLyP101–plasmid DNA complexes retained substantial binding activity, with an apparent dissociation constant ($K_d$) of 27 nM (Figure 2 and see Ref. 12) comparable to that of peptide P101 alone.[15] The fact that binding of importin to pLy or pLyP101T was abolished when complexed to plasmid DNA at a Ly/Nu of 0.4 implied that importin binding in its absence was through a nonspecific charge interaction which was eliminated upon neutralisation of the positive charge of the pLy backbone by the negatively charged DNA. That pLyP101 complexed with DNA retained the ability to be recognised by importin indicated that NLSs were accessible even when the pLy backbone was conjugated with DNA, representing the basis of enhancement of transfection (see Figure 1) above that of pLy and pLyP101T at a Ly/Nu ratio of 0.4.

Experiments over a range of different Ly/Nu ratios were consistent with the idea that recognition of pLy and pLyP101T in the absence of DNA by mIMPα/β was due to nonspecific charge interaction which was abolished upon addition of the negatively charged DNA. In contrast, pLyP101 exhibited substantial binding at all Ly/Nu ratios (see Figure 2). As the Ly/Nu ratio increased, the binding affinities and maximal binding of all three DNA–pLy conjugate complexes improved, with pLyP101–DNA being consistently and substantially better than both pLy–DNA and pLyP101T–DNA. When the Ly/Nu ratio was increased past 4.0, however, the binding of all three DNA complexes rose to levels comparable to those in the absence of DNA, presumably as a consequence of the positively charged pLy backbone being in excess.

Measurement of the *in vitro* nuclear import kinetics of FITC-labelled pLy, pLyP101 and pLyP101T in the absence or presence of complexed plasmid DNA indicated that pLyP101 accumulated in the nucleus to maximal levels almost 50% higher than those of pLyP101T, with poor nuclear accumulation of pLyP101T-DNA complexes at a Ly/Nu of 0.4 (Figure 3, and see Ref. 12). Exclusion of pLy–DNA complexes at the Ly/Nu of 0.4 from the nucleus was observed. Also, the increased rate of nuclear accumulation of pLyP101–DNA, as compared with that of pLyP101 alone implied a pLyP101-mediated nuclear cotransport of the complexed plasmid DNA, with the increase consistent with the idea that compaction of the DNA by pLy in the conjugates contributed to more efficient transport.[12] The maximal accumulation for DNA–pLy derivatives at the Ly/Nu ratio of 4.0 was not significantly different (Figure 3), in contrast to maximal accumulation at a Ly/Nu ratio of 0.4.

### *Dependence of structure of pLy–DNA on Ly/Nu*

To determine if pLy's ability to enhance DNA uptake was attributable to structural changes as a result of condensation, EM and AFM were used to visualise pLy–DNA

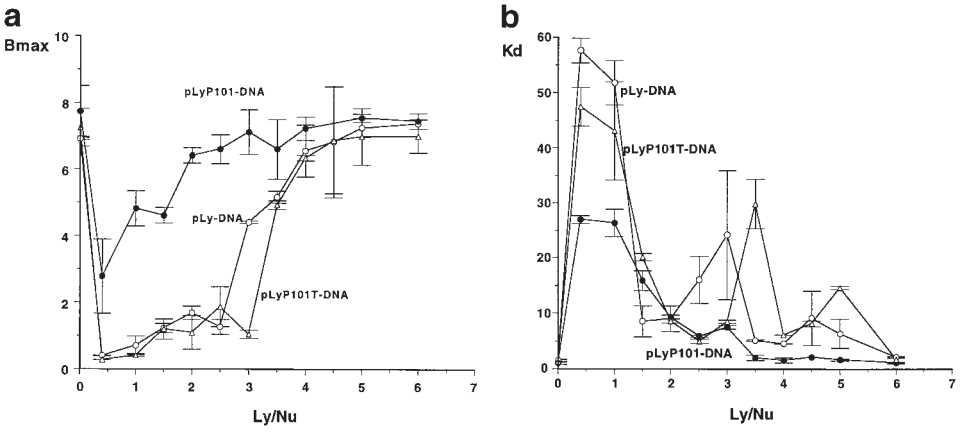


***Figure 2*** *Dependence on Ly/Nu of the recognition of DNA–pLy complexes by importin subunits. Importin binding to DNA–pLy conjugates was quantified using an ELISA assay as described in Materials and methods. pLy, pLyP101 or pLyP101T precomplexed with plasmid DNA at the respective Ly/Nu ratios were hybridised with increasing concentrations of mIMP α/β and quantification carried out as described in Materials and methods. Experimental data was then fitted for the function* $B(x) = B_{max}(1-e^{-kx})$*, where x is the concentration of importin, and Bmax is maximal binding. The dependence of Bmax (a) and the apparent dissociation constant ($K_d$, the importin concentration giving half maximum binding) (b) on the Ly/Nu ratio is shown. Results represent the mean ± s.e.m. (n ⩾ 3).*

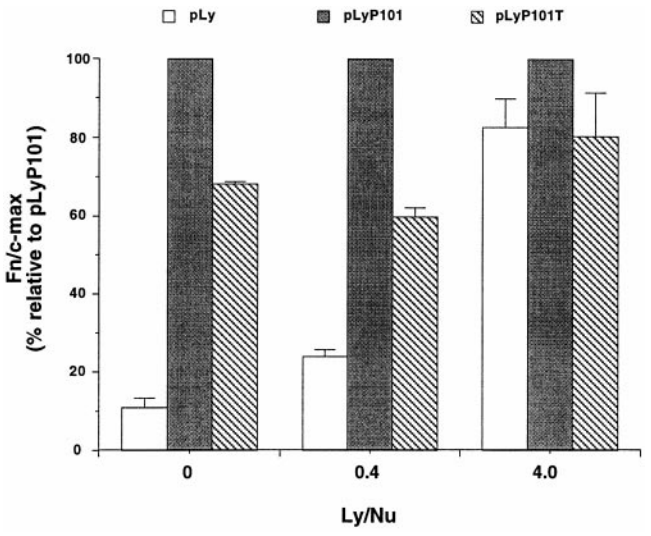


***Figure 3*** *Nuclear accumulation of pLy derivatives complexed with plasmid DNA at different Ly/Nu ratios. pLy, pLyP101 and pLyP101T were labelled with FITC, complexed with plasmid DNA at the Ly/Nu ratios indicated, and added to mechanically perforated HTC cells in the presence of an ATP-regenerating system and exogenous cytosol at room temperature as described in Materials and methods.[29,30] Nuclear import was visualised using CLSM and quantification performed by image analysis of the digitised images up to 40 min. The data were then fitted for* $Fn/c(t) = Fn/c_{max}\ (1-e^{-kt})$*, and maximal nuclear accumulation* ($Fn/c_{max}$) *expressed as a percentage relative to pLyP101 at the Ly/Nu ratio indicated. Results are for the mean ± s.e.m.* ($n \geqslant 3$).

complexes at different Ly/Nu ratios. EM results of free open circular plasmid DNA molecules (7174 bp) indicated a length of 2562 ± 45 nm, $n = 5$ (Figure 4 left top panel). At a Ly/Nu ratio of 0.4, the pLy–plasmid DNA complex revealed a tight toroid structure (diameter of *c*. 60 nm, see Table 1),[1] in contrast to the very large open plasmid structure in the absence of pLy (Figure 4, top left panel). A similar structure was also observed for the

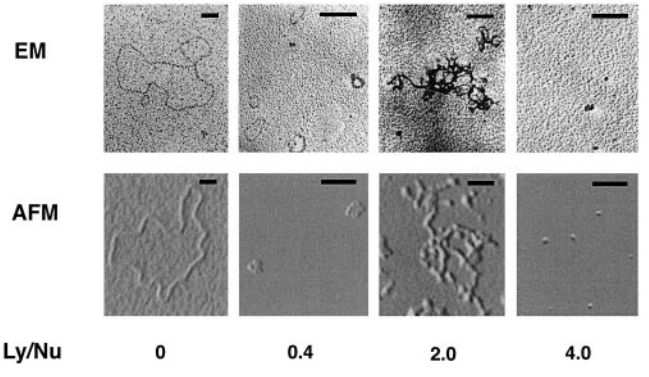


***Figure 4*** *Electron (top) and atomic force micrographs (bottom) of plasmid DNA with and without precomplexation with pLy at the Ly/Nu ratios indicated. For EM, samples were prepared, rotary shadowed and viewed as described in Materials and methods. Original magnifications used were 25000 (no pLy, left panels) and 45000 times (all other panels). For AFM images of pLy complexed with plasmid DNA (7.2 kb) at the Ly/Nu ratios indicated, pLy and plasmid DNA were complexed in HBS buffer as described in Materials and methods and 10 μl of each sample was added to freshly cleaved mica, allowed to sit for 5 min, washed with* $H_2O$ *and dried with a stream of compressed air. Complexes were imaged using the tapping mode in air. The images are flattened. In all cases, the scale bars represent 100 nm.*

pLyP101–DNA complex at a Ly/Nu ratio of 0.4 (diameter of 57 nm) (see Table 1). When the Ly/Nu ratio was increased to 2.0, aggregated matrixes were observed for both pLy–DNA and pLyP101–DNA with sizes varying from 150 to 800 nm (see Figure 4; Table 1). The structures for pLy–DNA were very similar to those of pLyP101–DNA, with aggregated complexes evident for both, indicative of the fact that the presence of NLSs, at least at the cross-linking ratio used, does not influence pLy's DNA compaction properties. At a ratio of 4.0, circular, tightly collapsed beads were observed for both pLy–DNA and pLyP101–DNA complexes (diameters of *c*. 17 and 15 nm, respectively – see Figure 4, top right; Table 1).

All results were confirmed using AFM in which a scanning tip was employed in tapping mode[16,17] to image the pLy– and pLyP101–DNA complexes for the first time. Figure 4 (bottom) illustrates the Ly/Nu ratio-dependent effect on pLy–DNA structures, demonstrating that pLy-induced DNA condensation involves defined structural intermediates progressing from an open circular plasmids to toroids, to aggregated meshwork, to a final collapse to tightly compact circular particles. As above, the pLyP101–DNA structures were similar to those of pLy–DNA (see also below), indicating that the NLSs do not impair the ability of pLy to compact DNA. Measurements of the size of free plasmid DNA (diameter of 2423 ± 54 nm, $n = 5$) and toroids at Ly/Nu of 0.4 for pLy–DNA and pLyP101–DNA (diameters of *c*. 63 and 60 nm, respectively) and collapsed beads at Ly/Nu of 4.0 (diameters of *c*. 19 and 15 nm, respectively), were consistent with the results from EM (see Table 1). AFM also allowed measurement of the thickness and contours of the respective structures, results indicating the thickness of open plasmid DNA to be 0.32 ± 0.04 nm ($n = 5$) in contrast to the toroids of pLy and pLyP101 at a Ly/Nu ratio of 0.4 (thicknesses of *c*. 3.1 and 2.9 nm, respectively) and the compacted particles of pLy and pLyP101 at Ly/Nu = 4.0 (thicknesses of 2.7 and 2.4 nm, respectively, see Table 1, Figure 5). The great variation of sizes and higher order structures presumably impact upon the ability of the complexes to be imported into the nucleus (see Ref. 12).

## Discussion

Functional NLS-containing peptides within pLy–DNA complexes can enhance transfection through their ability to be recognised by the cellular nuclear import machinery and importins in particular, and thereby mediate efficient nuclear targeting.[12] The ability of pLyP101 to enhance gene transfer as compared with pLy or pLyP101T was confirmed here using calcium phosphate as well as lipofectamine transfection. Figure 6 summarises data for the three parameters: transfection, importin binding and size in relation to the Ly/Nu ratio. It is clear that the size of transfecting conjugates, modulated through pLy's DNA-compacting properties, can be a critical factor for nuclear entry. In particular, the results indicate that the formation of large irregular complex aggregates at a Ly/Nu of 2.0 most probably explain the decrease in transfection efficiency of pLy conjugates at that ratio. At Ly/Nu ratios above 4.0, the requirement for a conventional NLS for efficient transfection is reduced, consistent with the idea that physically smaller conjugates do not appear to have as stringent a requirement for NLSs for nuclear import

**Table 1** Dimensions of pLy–DNA and pLyP101–DNA complexes formed at different Ly/Nu ratios as determined using EM and AFM

| *Ly/Nu ratio* | *Morphology* | *Average diameter (nm)* | | | |
|---|---|---|---|---|---|
| | | *EM* | | *AFM* | |
| | | *pLy–DNA* | *pLyP101–DNA* | *pLy–DNA* | *pLyP101–DNA* |
| 0.4 | 40–80 mm toroids | 60.8 ± 6.6 (6)[a] | 57.2 ± 6.4 (6)[a] | 62.5 ± 8.9 (5)[a,b] | 60.4 ± 5.3 (5)[a,c] |
| 2.0 | 150–800 nm meshwork | diverse shapes and sizes | diverse shapes and sizes | diverse shapes and sizes | diverse shapes and sizes |
| 4.0 | 12–20 nm collapsed beads | 17.1 ± 3.5 (6)[a] | 15.0 ± 2.9 (6)[a] | 19.3 ± 2.5 (8)[a,d] | 14.6 ± 3.5 (8)[a,e] |

[a]*n* in parentheses.
[b]Thickness measurement = 3.08 ± 0.96 nm.
[c]Thickness measurement = 2.88 ± 0.80 nm.
[d]Thickness measurement = 2.65 ± 0.40 nm.
[e]Thickness measurement = 2.44 ± 0.20 nm.

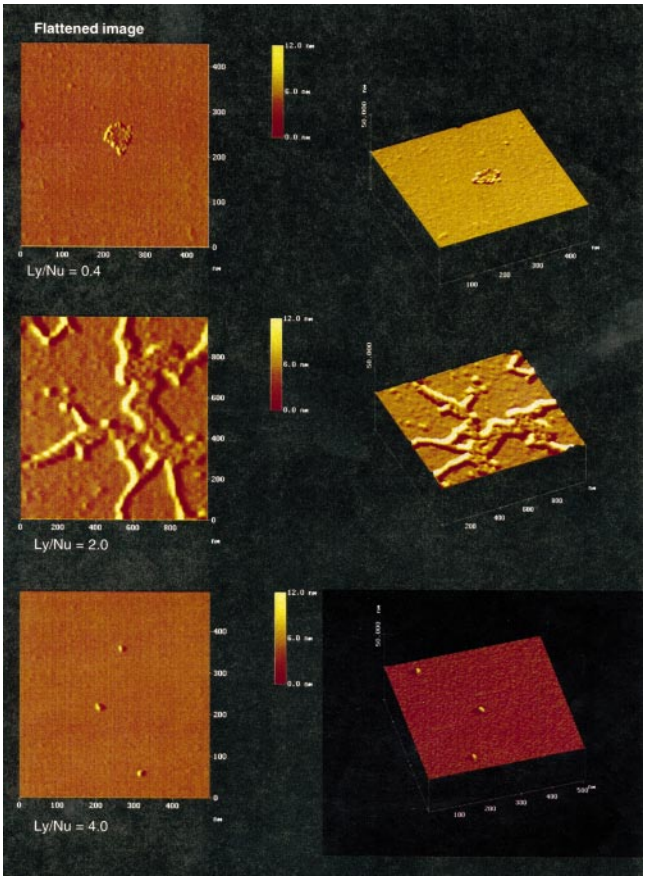


***Figure 5*** *AFM images of pLyP101 complexed with plasmid DNA at the Ly/Nu ratios indicated. pLyP101 and DNA were complexed as described in Materials and methods, adsorbed on to freshly cleaved mica and imaged in air as per Figure 4. Panels on the left show flattened images while panels on the right are angled to emphasize topography.*

as larger ones.[18] Importantly as highlighted in Figure 6, at a Ly/Nu ratio of 2.0, transfection efficiency is low even for pLyP101–DNA, despite high importin binding affinity, implying that the size factor is more important for gene transfer under these conditions than importin recognition. Dimensions obtained for open plasmids and toroids corresponded well with the estimates of others.[16,17] The progressive collapse of pLy–DNA structures due to the increasing Ly/Nu ratio observed here parallels that found by salt-dependent pLy–DNA complex formation,[8,10] an important observation being that NLSs appear not to affect pLy's DNA compaction ability.

This is the first time AFM has been used to visualise the Ly/Nu ratio stage-like collapse of plasmid DNA when complexed with NLS-containing pLy conjugates, supporting the finding that NLSs appear not to affect pLy-mediated DNA compaction. Consistent with the observations of others,[1] our EM and AFM analysis both indicate that the diameter of the NLS-containing transfecting constructs used at a Ly/Nu ratio of 0.4 (*c.* 60 nm) is greater than the maximum (*c.* 27 nm) for NLS-mediated nuclear transport determined using gold particles as inert carriers.[18,19] Since enhanced transfection and nuclear import is observed in our study, as well as that of Wagner and co-workers,[1] and many others, it can only be concluded that, unlike gold particles, pLy conjugates possess sufficient flexibility to enable them to pass through the nuclear pore complex and into the nucleus.

As shown in Figure 6, the biggest effective enhancement of the gene transfer by the NLS peptide relative to that conferred by the non-functional NLS peptide (50–60%), occurs at a Ly/Nu ratio of 0.4. As the advantage conferred by the reduction in the size of the complexes overrides the benefit of nuclear targeting at a Ly/Nu ratio of 4.0, there is no longer a significant difference between conjugates with or without a functional NLS. The fact that functional NLSs may not be required for enhancement of transfection if an excess of pLy is used, is consistent with recent observations regarding pLy-mediated enhancement of transfection.[20,21] The nuclear pore complex has been visualised using EM and found to have a central pore or diaphragm with an open channel of 9 nm[22] which correlates with the pore size estimated from diffusion measurements.[23] The pLy–DNA complexes at a Ly/Nu ratio of 4.0 (*c.* 15.0 nm, see Table 1), with sufficient flexibility (see Ref. 12), may thus be small enough to be able to pass through the nuclear pore by diffusion. In this study, the NLS-containing peptide that was cross-linked to pLy was most effective at a Ly/Nu ratio of 0.4. (Figure 6), whereas plasmid DNA, when complexed with pLy at a Ly/Nu ratio of 4.0, has the advantage of tight compaction that facilitates nuclear

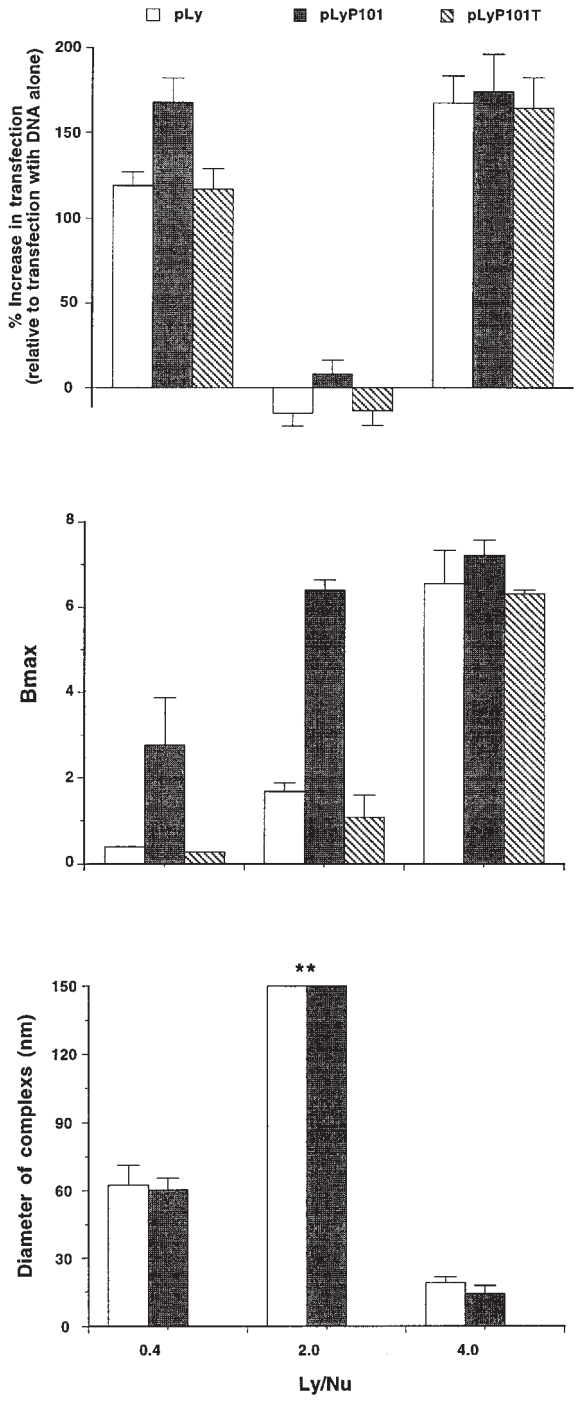


***Figure 6*** *Correlation of transfection enhancement, maximal importin α/β binding and structure of pLy, pLyP101– and pLyP101T–DNA according to the Ly/Nu ratio. Stable transfection using the calcium phosphate procedure with pLy- and pLyP101–DNA complexes at Ly/Nu ratios of 0.4, 2.0 and 4.0 was carried out as described in Materials and methods and the enhancement of transfection expressed as the percentage increase compared with transfection with plasmid DNA alone. Maximal binding to importin α/β of pLy- and pLyP101- to DNA complexes at the different Ly/Nu ratios was obtained from ELISA binding assays (see Figure 2) while the diameters of complexes were measured using AFM (see Figure 4 and Table 1). Complexes at a Ly/Nu ratio of 2.0 (**) were aggregates larger than 150 nm (see also Figures 3 and 4).*

entry in contrast to complexation at Ly/Nu of 2.0. Thus, an important finding from this study is that it is critical to use pLy/pLy–NLS conjugates at an optimal Ly/Nu ratio to ensure maximal nuclear accumulation and thereby gene transfer.

## Materials and methods

### *Cross-linking of NLS peptides to pLy*

P101, a peptide (CGPGSDDEAAADAQHAAPPKKK RKVGY) harbouring the T-ag NLS (PKKKRKV[132]) together with the flanking nuclear import-enhancing protein kinase CK2 phosphorylation site (S[112]DDE), and P101T a peptide (CGPGSDDEAAADAQHAAPPKt KRKVGY) which contains the mutant Thr[128] substituted form of the T-ag NLS were cross-linked to pLy (molecular mass 110 kDa; Sigma, St Louis, MO, USA) to give pLyP101 and pLyP101T, respectively, using the heterobifunctional cross-linker N-succinimidyl 3-(2-pyridyldithio)propionate (SPDP).[12,24] pLyP101 carries 30.1 P101 peptides on average, while pLyP101T has 31.8 P101T peptides.

### *pLy–DNA complexation*

DNA–pLy complexation was carried out by adding 2 μg of plasmid DNA (6.2 kb) to various amounts of pLy, pLyP101 or pLyP101T in a final volume of 100 μl HBS buffer (Hepes-buffered saline: 150 mM NaCl, 20 mM Hepes, pH 7.4) to obtain a range of Ly/Nu ratios, vortexed for 10 s, and incubated for 30 min at room temperature before use.[12,24] Complexation was routinely monitored by gel electrophoresis.[3,9,25]

### *DNA transfection*

Calcium phosphate transfection was performed using a protocol modified from that of Okayama and Chen.[26] HTC (rat hepatoma) cells were trypsinised, seeded in DMEM/10% FCS in six-well costars (Nunclon, Denmark) at a density of $2 \times 10^5$ cells per well and incubated overnight in 5% $CO_2$ atmosphere at 37°C. Reporter plasmids were complexed as described above with various amounts of pLy, pLyP101, pLyP101T before the addition of 125 mM $CaCl_2$, and 2× BES buffer (50 mM BES pH 6.95, 280 mM NaCl, 1.5 mM $Na_2HPO_4$). The mixture was left for 10 min at room temperature before being added drop-wise to cells as previously.[27]

For lipofectamine transfection, $2 \times 10^5$ cells in 2 ml of DMEM/10% FCS were seeded per well in a six-well plate (Falcon, Becton Dickinson, Franklin Lakes, NJ, USA) and incubated at 37°C in 5% $CO_2$ for 24 h to obtain 70–80% confluence. Fifteen μg plasmid DNA complexed with various amounts of pLy, pLyP101 or pLyP101T was diluted in 1.5 ml serum-free medium to obtain a DNA solution of 1 μg/100 μl (solution A). Six μl of LipofectAMINE (Gibco, Life Technologies, Melbourne, Australia) was added to 100 μl serum-free medium in a sterile Eppendorf tube and incubated at room temperature for 30 min (solution B). One hundred μl of solution A was added to solution B in each tube, mixed gently and incubated at room temperature for 30 min to allow formation

of the DNA–liposome complex. Eight hundred μl of serum-free medium was then added to the DNA–lipid complex solution and the diluted mixture added to the cells. After incubation at 37°C in 5% $CO_2$ for 5 h, 1 ml of medium containing 20% FCS was added to each well.

Irrespective of whether calcium phosphate or lipofection methods were used, transient transfection was analyzed 48 h after transfection with plasmid pCH110,[14] encoding the *E. coli* β-galactosidase enzyme by assaying for β-galactosidase activity using the Galacto-light Plus chemiluminescence assay.[27] In the case of stable transfection, plasmid pSV2neo[13] encoding the neomycin resistance gene was used, and G418 antibiotic (neomycin, Gibco, Life Technologies) added 48 h after transfection. Resistant colonies were counted after 10 days.[27]

### *Binding affinities of pLy–DNA complexes*

Recognition of pLy, pLyP101 and pLyP101T–DNA by mIMPα/β, expressed as glutathione-S-transferase (GST) fusion proteins in *E. coli* was quantified using an enzyme-linked immunosorbent assay (ELISA)-based assay.[15] As previously, pLy, pLyP101 or pLyP101T (5 pmol per well) precomplexed with DNA at different Ly/Nu ratios were added to 96-well microtitre plates, hybridized with increasing concentrations of mIMPα/β, and bound importin determined as described.[12,15,28]

### *Labelling of pLy and pLy derivatives and in vitro nuclear transport assay*

Fluorescein-5-isothiocyanate (FITC) labelling of pLy and its derivatives was carried out as previously.[12] To determine nuclear import kinetics, the labelled pLy derivatives, subsequent to precomplexation with or without DNA, were added to mechanically perforated HTC cells together with cytosolic extracts (untreated reticulocyte lysate) and an ATP-regenerating system.[12,29,30] CLSM imaging, analysis and curve fitting was carried out as previously.[12,28,30]

### *EM and AFM*

Plasmid DNA and its complexes with pLy and pLyP101 at various Ly/Nu ratios were prepared for EM and rotary shadowing as previously.[12,31] For AFM, pLy and pLyP101–plasmid DNA complexes at various Ly/Nu ratios were diluted with HBS to a final DNA concentration of 10 ng/μl. Ten μl of each sample were added to freshly cleaved mica (1.5 $cm^2$), allowed to sit for 5 min and washed three times with 100 μl of $H_2O$ before drying with a stream of compressed air.[17] Tapping mode AFM was carried out with a MultiMode AFM and Nanoscope III (Digital Instruments, Santa Barbara, CA, USA), scanning at a rate of 1–2 Hz with a 125 μm silicon cantilever (Digital Instruments) oscillating at 400 Hz. Images were processed by flattening or angled to emphasise topography and analysed using the Nanoscope software v3.12.

## References

1 Wagner E, Cotten M, Foisner R, Birnstiel ML. Transferrin-polycation–DNA complexes: the effect of polycations on the structure of the complex and DNA delivery to cells. *Proc Natl Acad Sci USA* 1991; **88**: 4255–4259.
2 Wu GY, Wu CH. Receptor mediated gene delivery and expression *in vivo*. *J Biol Chem* 1988; **263**: 14621–14624.
3 Hart SL *et al*. Gene delivery and expression mediated by an integrin-binding peptide. *Gene Therapy* 1995; **2**: 552–554.
4 Rosenkranz AA *et al*. Receptor-mediated endocytosis and nuclear transport of a transfecting DNA construct. *Exp Cell Res* 1992; **199:** 323–329.
5 Ferkol T, Perales JC, Mularo F, Hanson RW. Receptor-mediated gene transfer into macrophages. *Proc Natl Acad Sci USA* 1996; **93**: 101–105.
6 Sosnowski BA *et al*. Targeting DNA to cells with basic fibroblast growth factor (FGF2). *J Biol Chem* 1996; **271**: 33647–33653.
7 Baeza I *et al*. Electron microscopy and biochemical properties of polyamine-compacted DNA. *Biochemistry* 1987; **26**: 6387–6392.
8 Perales JC *et al*. Gene transfer *in vivo*: sustained expression and regulation of genes introduced into the liver by receptor-targeted uptake. *Proc Natl Acad Sci USA* 1994; **91**: 4086–4090.
9 Vitiello L *et al*. Condensation of plasmid DNA with polylysine improves liposome-mediated gene transfer into established and primary muscle cells. *Gene Therapy* 1996; **3**: 396–404.
10 Perales JC *et al*. Biochemical and functional characterization of DNA complexes capable of targeting genes to hepatocytes via the asialoglycoprotein receptor. *J Biol Chem* 1997; **272**: 7398–7407.
11 Ziady AG *et al*. Chain length of the polylysine in receptor-targeted gene transfer complexes affects duration of reporter gene expression both *in vitro* and *in vivo*. *J Biol Chem* 1999; **274**: 4908–4916.
12 Chan CK, Jans DA. Enhancement of polylysine-mediated transferrinfection by nuclear localization sequences: polylysine does not function as a nuclear localization sequence. *Hum Gene Ther* 1999; **10**: 1695–1702.
13 Southern PJ, Berg P. Transformation of mammalian cells to antibiotic resistance with a bacteria gene under control of the SV40 early region promoter. *J Mol App Gen* 1982; **1**: 327–341.
14 Hall CV, Jacob PE, Ringold GM, Lee F. Expression and regulation of *Escherichia coli lacZ1* gene fusions in mammalian cells. *J Mol Appl Genet* 1983; **2**: 101–109.
15 Hubner S, Xiao CY, Jans DA. The protein kinase CK2 site (Ser111/112) enhances recognition of the simian virus 40 large T-antigen nuclear localization sequence by importin. *J Biol Chem* 1997; **272**: 17191–17195.
16 Bustamante C *et al*. Circular DNA molecules imaged in air by scanning force microscopy. *Biochemistry* 1992; **31**: 22–26.
17 Hansma HG *et al*. DNA condensation for gene therapy as monitored by atomic force microscopy. *Nucleic Acids Res* 1998; **26**: 2481–2487.
18 Feldherr CM, Akin D. EM visualization of nucleocytoplasmic transport processes. *Electron Microsc Rev* 1990; **3**: 73–86.
19 Feldherr CM, Akin D. The location of the transport gate in the nuclear pore complex. *J Cell Sci* 1997; **110**: 3065–3070.
20 Page RL *et al*. Transgenesis in mice by cytoplasmic injection of polylysine/DNA mixtures. *Transgenic Res* 1995; **4**: 353–360.
21 Pollard H *et al*. Polyethylenimine but not cationic lipids promotes transgene delivery to the nucleus in mammalian cells. *J Biol Chem* 1998; **273**: 7507–7511.
22 Goldberg MW, Allen TD. High resolution scanning electron microscopy of the nuclear envelope: demonstration of a new, regular, fibrous lattice attached to the baskets of the nucleoplasmic face of the nuclear pores. *J Cell Biol* 1992; **119**: 1429–1440.
23 Akey CW. Visualization of transport-related configurations of the nuclear pore transporter. *Biophys J* 1990; **58**: 341–355.
24 Wagner E *et al*. Transferrin–polycation conjugates as carriers for DNA uptake into cells. *Proc Natl Acad Sci USA* 1990; **87**: 3410–3414.
25 Ma C, Bloomfield VA. Condensation of supercoiled DNA induced by MnCl2. *Biophys J* 1994; **67**: 1678–1681.
26 Okayama H, Chen C. In M Ej (ed). *Methods in Molecular Biology, Vol 7: Gene Transfer and Expression protocols*. Humana Press: Clifton, NJ, 1991, pp 15–21.
27 Chan CK, Hubner S, Hu W, Jans DA. Mutual exclusivity of DNA binding and nuclear localization signal recognition by the yeast transcription factor GAL4: implications for nonviral DNA delivery. *Gene Therapy* 1998; **5**: 1204–1212.

28 Xiao CY, Hubner S, Jans DA. SV40 large tumor antigen nuclear import is regulated by the double-stranded DNA-dependent protein kinase site (serine 120) flanking the nuclear localization sequence. *J Biol Chem* 1997; **272**: 22191–22198.
29 Jans DA *et al*. $p34^{cdc2}$-mediated phosphorylation at $T^{124}$ inhibits nuclear import of SV40 T-antigen proteins. *J Cell Biol* 1991; **115**: 1203–1212.
30 Xiao CY *et al*. A consensus cAMP-dependent protein kinase (PK-A) site in place of the CcN motif caesin kinase II site of Simian virus 40 large T-antigen confers PK-A mediated regulation of nuclear import. *J Biol Chem* 1996; **271**: 6451–6457.
31 Tyler JM, Branton D. Rotary shadowing of extended molecules dried from glycerol. *J Ultrastruct Res* 1980; **71**: 95–102.